Imager Processing : Data Dictionary

Nicolas Clerbaux

28 July 2006

MSG-RMIB-GE-TN-0024

Abstract

This document describes the various constants, parameters, models, ... used within the imager processing (also called 'SEVIRI processing') part of the RMIB GERB Processing (RGP) at RMIB.

Contents

1 Introduction

Scope of this document

This document describes the various constants, parameters, models, ... used within the imager processing (also called 'SEVIRI processing') part of the RMIB GERB Processing (RGP) at RMIB.

The document also contains data related to Meteosat First Generation as the long-lasting series of MFG measurement could be of interest for climate monitoring of the Earth radiation Budget.

Related documents

The related design and algorithm development documents are: [TN05], [TN07], [TN08] and [TN30].

Localisation of the data

Most of the data described in this document are available to the RMIB GERB team on our file server tsunami in the directory $DATA:

```
DATA=/tsunami/gerb/Data
```

2 Radiative Transfer Models

SBDART

This freeware radiative transfer model is not used in real time but has been used intensively to derive some data and models necessary for the imager processing. The software is described in [TN30] and the source (in Fortran) can be downloaded via the web site:

`http://www.crseo.ucsb.edu/esrg/pauls_dir`

On SGI, don't forget to force the REAL type to be 8 bytes when compiling the model. The best result are obtained using SBDART on a DEC alpha computer (which was used to develop and test the software!). SBDART has been used to generate a data base of spectral radiance fields at the TOA. The generation of this database is described in [TN30]. This database has been used to parameterize the spectral modeling part of the processing and the radiance-to-flux conversion for the thermal radiation. The first version of the database has been built using the SBDART version 2.1. This first version includes shortwave and longwave simulations. In a second step, a second version of the database has been generated using the SBDART version 2.4. This second version contains only shortwave simulations.

STREAMER

The STREAMER radiative transfer model has been used to parameterize the look-up-tables used for the cloud identification. The Version 3 of this RTM has been used.

MODTRAN

MODTRAN 3.7 was used, but only for validation purpose. So, the processing is not dependent on this software.

3 Meteosat spectral response curves

This data is of prime importance because the spectral modeling parameters are directly dependent on it. The spectral response curves for the Meteosat-[5,6,7,8,9,10] have been downloaded from the EUMETSAT web site

```
http://www.eumetsat.de
```

and are stored in separate ASCII files for each channel $(\lambda[\mu m], \phi(\lambda))$ in the directories:

```
$DATA/SpectralResponse/MS5
$DATA/SpectralResponse/MS6
$DATA/SpectralResponse/MS7
$DATA/SpectralResponse/SEV1
$DATA/SpectralResponse/SEV2
$DATA/SpectralResponse/SEV3
```

For each curve the Filter Integral (FI and FI') value are evaluated in $[\mu m]$ and in $[cm-1]$. The central wavelength λ_s is also evaluated. The different values are given in Tab.(1). The equations are (with $w = 10000/\lambda$):

$$FI[\mu m] = \int \phi_{ch}(\lambda) d\lambda \quad (1)$$

$$FI'[cm^{-1}] = \int \phi_{ch}(w) dw \quad (2)$$

$$\lambda_s = \frac{\int \lambda \phi_{ch}(\lambda) d\lambda}{\int \phi_{ch}(\lambda) d\lambda} \quad (3)$$

Meteosat First Generation

For Meteosat-5,-6,-7, there are 2 visible detectors (VIS1 and VIS2). The averaged curve for the 2 detectors is used in the processing. The Fig.(1) illustrates the spectral response curves for MS-5,-6,-7.

The Fig.(2) shows a comparison of the visible channels. One can see that the spectral sensitivity of the Meteosat-5 and -6 satellites are similar. On the other hand, the Meteosat-7 spectral response is quite different. According to Yves Govaerts, the characterization of the MS-5 and MS-7 visible channel sensitivity is probably wrong and one does better to use MS-7 curves for the MS-5 and MS-6 satellites.

Meteosat Second Generation

The SEVIRI spectral response curves are given on figures (3). Note that for the thermal channels, the SR at the nominal focal plane temperature ($95K$) has been selected. The curves at $85K$ have also been downloaded but should not be used. For the HRV channel an extended curves over $[0.3 : 1.3]\mu m$ is also available.

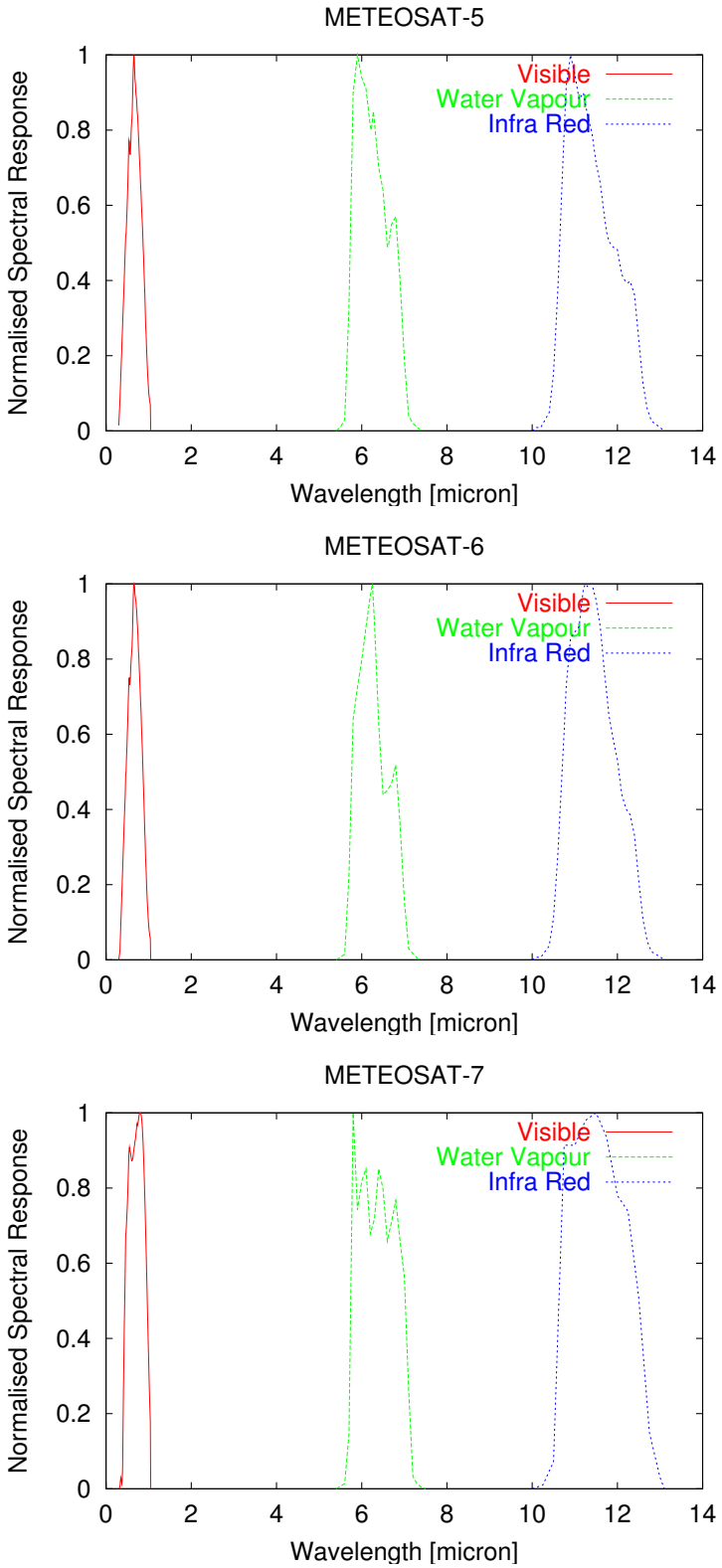

Figure 1: Spectral response curves for the Meteosat-5 (top), -6 (center) and-7 (bottom) radiometers. The visible channel refers to the average VIS1 and VIS2 detectors.

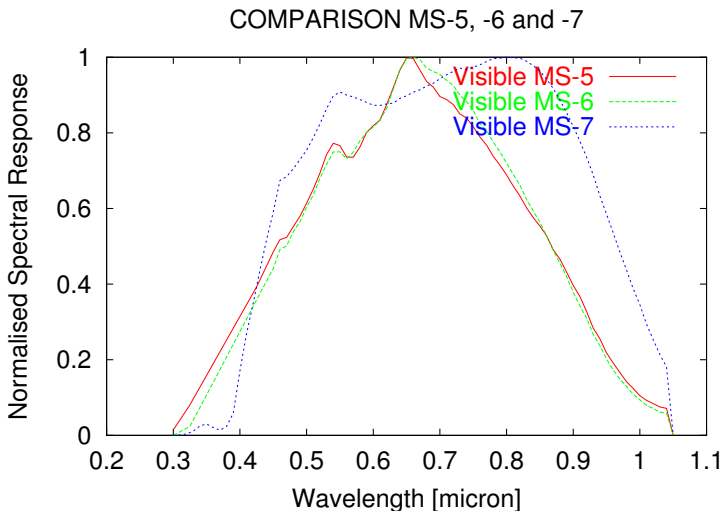

Figure 2: Comparison of the visible channel spectral responses for the Meteosat-5, 6 and 7 satellite.

```
$DATA/SpectralResponse/SEV1/SR_SEV1_HRV.txt
$DATA/SpectralResponse/SEV1/SR_SEV1_HRV_extended.txt
$DATA/SpectralResponse/SEV1/SR_SEV1_VIS006.txt
$DATA/SpectralResponse/SEV1/SR_SEV1_VIS008.txt
$DATA/SpectralResponse/SEV1/SR_SEV1_IR_016.txt
$DATA/SpectralResponse/SEV1/SR_SEV1_IR_039.txt
$DATA/SpectralResponse/SEV1/SR_SEV1_WV_062.txt
$DATA/SpectralResponse/SEV1/SR_SEV1_WV_073.txt
$DATA/SpectralResponse/SEV1/SR_SEV1_IR_087.txt
$DATA/SpectralResponse/SEV1/SR_SEV1_IR_097.txt
$DATA/SpectralResponse/SEV1/SR_SEV1_IR_108.txt
$DATA/SpectralResponse/SEV1/SR_SEV1_IR_120.txt
$DATA/SpectralResponse/SEV1/SR_SEV1_IR_134.txt
```

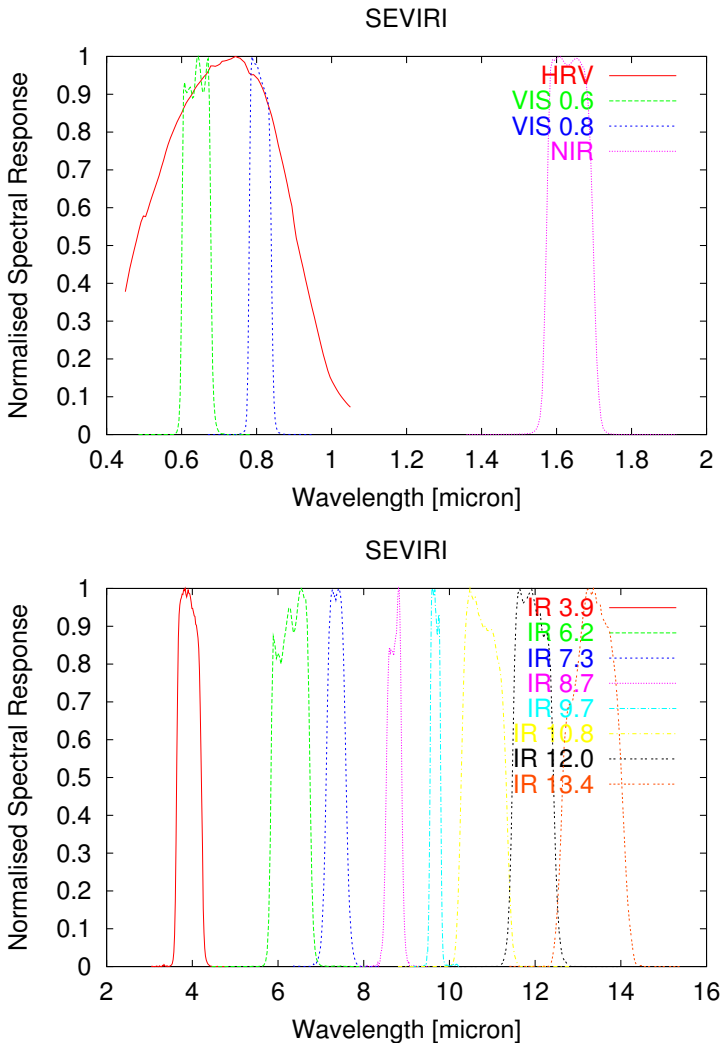

Figure 3: SEVIRI PFM (instrument on MSG-1 or 'SEV1') spectral response curves for solar (top) and thermal (bottom) channels.

4 GERB Averaged Spectral Response curves

The spectral response of the GERB instrument must be known because the imager processing has to estimate the broadband filtered radiances that would have been measured by the GERB radiometer.

The TOT and SW spectral response curves for the 256 detectors of the GERB instruments are provided by Imperial College. For each detector the A factor is evaluated using a Planck's curve $L_{5800K}(\lambda)$ for a blackbody at $5800K$:

$$A = \frac{\int \phi_{TOT}(\lambda) L_{5800K}(\lambda) d\lambda}{\int \phi_{SW}(\lambda) L_{5800K}(\lambda) d\lambda} \tag{4}$$

The (synthetic) LW spectral response curves is then constructed for each detector as:

$$\phi_{LW}(\lambda) = \phi_{TOT}(\lambda) - A * \phi_{SW}(\lambda) \tag{5}$$

Finally, the average SW, LW and TOT curves are constructed by averaging the 256 curves.

GERB-2 Spectral Response

A first version of the GERB-2 spectral response curves has been used in the processing during a couple of years but have been reprocessed since then by IC. We do not describe anymore this data. The reprocessed version is labelled as '08072005' and is used for the GERB-2 Edition-1 data release. The averaged spectral response curves for the GERB-2 radiometer are stored in the following files and are illustrated on Fig.(4):

```
$DATA/SpectralResponse/GERB2/g2_sr_lw_08072005.txt
$DATA/SpectralResponse/GERB2/g2_sr_sw_08072005.txt
$DATA/SpectralResponse/GERB2/g2_sr_tot_08072005.txt
```

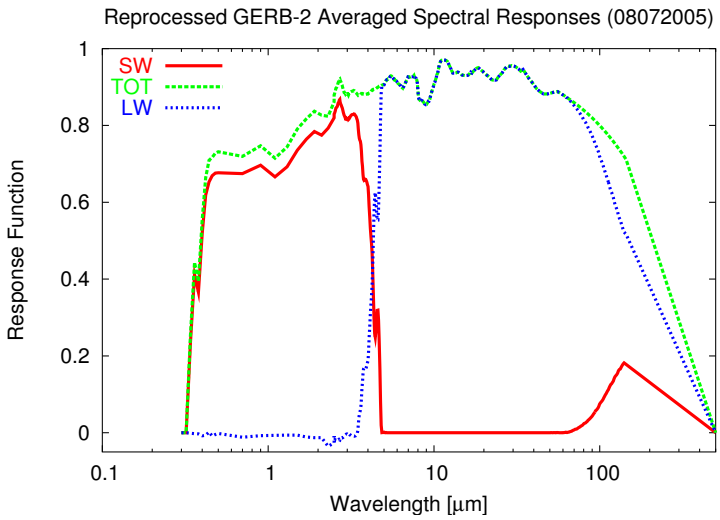

Figure 4: GERB-2 averaged 08072005 spectral response curves as used for the Edition-1.

5 Solar spectrum and NB solar radiances

Solar spectrum

The reference solar spectrum curve $F^{sol}(\lambda)$ used at RMIB is derived from the ATLAS-1 mission. This data is defined over the $[0.199 : 20]\mu$ range, is illustrated on Fig.(5) and is stored in the ASCII file $(\lambda[\mu m], F^{sol}(\lambda)[Wm^{-2}\mu^{-1}])$:

```
$DATA/RefSpectralCurves/solspec.txt
```

NB solar radiance

The NB solar radiance is needed to convert NB radiance into reflectance:

$$L_{ch}^{sol} = \frac{1}{\pi} \int F^{sol}(\lambda)\phi_{ch}(\lambda)d\lambda \tag{6}$$

channel	FI $[\mu m]$ Eq.(1)	FI' $[cm^{-1}]$ Eq.(2)	λ_s $[\mu m]$ Eq.(3)	L_{ch}^{sol} $[Wm^{-2}sr^{-1}$ Eq.(6)
G2 TOT	247.772403	20992.517577	167.998760	305.864777
G2 SW	42.108786	17612.257552	219.950225	282.477152
G2 LW	202.139010	1906.269487	156.271035	-0.251703
MS5 VIS	0.392077	10683.542467	0.664948	179.593528
MS6 VIS	0.387941	10218.346465	0.670132	178.030082
MS7 VIS	0.495095	11630.940046	0.710964	216.102204
SEV1 HRV	0.405763	8990.897822	0.712926	178.655155
SEV1 HRVext	0.421284	9675.452745	0.708220	185.424357
SEV1 VIS006	0.074485	1824.614643	0.640209	37.592432
SEV1 VIS008	0.057294	876.101219	0.809281	19.973203
SEV1 IR 016	0.125746	471.311575	1.634771	9.605848
SEV1 IR 039	0.558591	365.631468	3.920179	1.689679
SEV1 WV 062	0.848394	214.572920	6.306292	0.391023
SEV1 WV 073	0.478961	88.624939	7.356759	0.119576
SEV1 IR 087	0.345815	45.604889	8.710686	0.044722
SEV1 IR 097	0.249015	26.629038	9.671304	0.021411
SEV1 IR 108	0.974868	83.985849	10.788202	0.055471
SEV1 IR 120	0.937314	65.836404	11.942996	0.033702
SEV1 IR 134	1.252259	70.458815	13.351408	0.027414
SEV2 HRV	0.408572	9014.875790	0.714686	179.368883
SEV2 HRVext	0.422235	9752.687438	0.706424	186.420692
SEV2 VIS006	0.073384	1796.953050	0.640330	37.028792
SEV2 VIS008	0.057317	878.890906	0.808172	20.022596
SEV2 IR 016	0.125917	469.971389	1.638182	9.568981
SEV2 IR 039	0.571128	374.462112	3.917130	1.733285
SEV2 WV 062	0.854844	216.852941	6.296798	0.396279
SEV2 WV 073	0.467186	86.227821	7.365982	0.116039
SEV2 IR 087	0.344250	45.363315	8.714076	0.044456
SEV2 IR 097	0.239560	25.665639	9.662214	0.020675
SEV2 IR 108	1.008341	87.056153	10.776935	0.057589
SEV2 IR 120	0.988474	68.891516	11.989880	0.034828
SEV2 IR 134	1.212074	68.101955	13.360204	0.026431

Table 1: Main characteristics of the Meteosat and GERB filters used in the RGP.

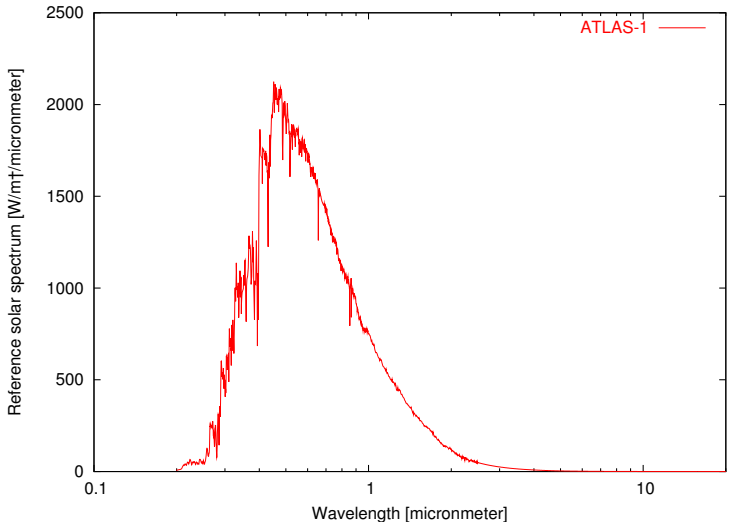

Figure 5: Reference solar spectrum used at RMIB.

6 Imager calibration

Meteosat First Generation

For Meteosat first Generation, the NB radiances are obtained as a linear transformation of the integer count value C provided in the 8-bits images:

$$L[Wm^{-2}sr^{-1}] = g(C - C_0) \tag{7}$$

where g is the **calibration coefficient** and C_0 is the the **space count**.

This information is available in the PIF/XPIF header for the WV and IR Meteosat images but not for the visible channel. For the visible channels of the Meteosat-5 and -7, we use a space count of 5 and a calibration coefficients that varies with the time linearly (drift):

$$g = g_0 * (1 + DN) \tag{8}$$

where $g_0$is the calibration for the launch date and N is the number of days since the launch.

For MS7, the launch date is 19970902 and we used the value $g_0 = 0.938$, $D = 6.63411\,10^{-5}$,$C_0 = 5$ which is just 0.03 higher than the Y. Govaerts values ($g_0 = 0.908$). Our value is obtained by cross calibration with the CERES instruments (on TRMM and Terra) as explained in the technical note [TN36].

Meteosat Second Generation

For the SEVIRI channels this information is provided in the XPIF header for all the channels but in a different form.

$$L[mWm^{-2}sr^{-1}(cm^{-1})^{-1}] = c_f C + L_0 \tag{9}$$

where c_f is given in $[mWm^{-2}sr^{-1}(cm^{-1})^{-1} \,/\, count]$ and L_0 is given in $[mWm^{-2}sr^{-1}(cm^{-1})^{-1}]$.

To convert these values into g and C_0 one uses:

$$g = 0.001 * c_f * FI' \tag{10}$$

$$C_0 = -L_0/c_f \tag{11}$$

where FI' is the filter integration in $[(cm^{-1})]$ as given in Tab.(1).

During the MSG1 commissioning in 2003 no calibration values were provided for the solar channels. In this case the following values provided by Yves Govaerts have been used:

channel	c_f	C_0
SEV1 HRV	0.0316	51
SEV1 VIS 006	0.0229	51
SEV1 VIS008	0.0302	51
SEV1 IR 016	0.0239	51

7 Radiance to brightness temperature conversion

Meteosat First Generation

The estimation of the brightness temperature $T_B\,[K]$ from the WV and IR NB radiance measurements $L\,[Wm^{-2}sr^{-1}]$ is performed using the exponential fit:

$$L = e^{A+\frac{B}{T_B}} \quad (12)$$

$$T_B = \frac{-B}{A - logL} \quad (13)$$

The regression coefficients for MS-5,-6,-7 are taken from the EUMETSAT calibration web page.

channel	A	$B[K]$
MS5 - WV2	9.2361	-2266.7 K
MS5 - IR1	6.7348	-1272.2 K
MS6 - WV2	9.1124	-2264.9 K
MS6 - IR1	6.7615	-1267.2 K
MS7 - WV1	9.2477	-2233.4882 K
MS7 - IR2	6.9618	-1255.5465 K

Meteosat Second Generation

For the SEV-1 thermal channels, Similar A and B coefficients have been estimated by A. Ipe at RMIB.

channel	A	$B[K]$
IR 3.9	12.2099	-3623.61 K
WV 6.2	9.19358	-2272.22 K
WV 7.3	7.88487	-1955.83 K
IR 8.7	6.72988	-1655.59 K
IR 9.7	5.89049	-1494.19 K
IR 10.8	6.72794	-1344.94 K
IR 12.0	6.20094	-1220.07 K
IR 13.4	5.96514	-1099.56 K

These values have been used in a first time. In a second time EUMETSAT provided an improved relation to estimate brightness temperature from radiance which takes the form:

$$T_B = \frac{1}{\alpha}\left(\frac{C_2\nu_c}{log\left(\frac{C_1\nu_c^3}{L[mWm^{-2}sr^{-1}(cm^{-1})^{-1}]}+1\right)}-\beta\right) \quad (14)$$

$$T_B = \frac{1}{\alpha}\left(\frac{C_2\nu_c}{log\left(\frac{1000}{FI'}L[Wm^{-2}sr^{-1}]+1\right)}-\beta\right) \quad (15)$$

$$C_1 = 1.1910410^{-5} mWm - 2sr - 1(cm-1)^{-4} \quad (16)$$

$$C_2 = 1.43877K(cm-1)^{-1} \quad (17)$$

The following values are provided on the EUMETSAT web site in a document from Stephen Tjemkes with title "On the Conversion from Radiances to Equivalent Brightness Temperatures".

Channel ID.	$\nu_c[cm-1]$	α	$\beta[K]$
SEV1 IR 039	2567.330	0.9956	3.410
SEV1 WV 062	1598.103	0.9962	2.218
SEV1 WV 073	1362.081	0.9991	0.478
SEV1 IR 087	1149.069	0.9996	0.179
SEV1 IR 097	1034.343	0.9999	0.060
SEV1 IR 108	930.647	0.9983	0.625
SEV1 IR 120	839.660	0.9988	0.397
SEV1 IR 134	752.387	0.9981	0.578
SEV2 IR 039	2568.832	0.9954	3.438
SEV2 WV 062	1600.548	0.9963	2.185
SEV2 WV 073	1360.330	0.9991	0.470
SEV2 IR 087	1148.620	0.9996	0.179
SEV2 IR 097	1035.289	0.9999	0.056
SEV2 IR 108	931.700	0.9983	0.640
SEV2 IR 120	836.445	0.9988	0.408
SEV2 IR 134	751.792	0.9981	0.561

8 Rectified Grid Parameters

The geostationary data are provided by EUMETSAT on rectified grids on a "satellite projection". The tables hereafter gives the grid parameters at the imager full resolution and at the 1/3 resolution (output grid) and for the BARG and ARG grids. When a grid is downsampled by a factor N (usually 3 or 15), the centers C_x and C_y are modified as:

$$c'_x = \frac{(c_x + 0.5)}{N} - 0.5 \quad (18)$$

$$col\_ang' = col\_ang * N \quad (19)$$

These parameters are stored in ASCII files in the directory:

```
$DATA/Grid/grid_${FORMAT}.txt
```

format	N	width height	C_x C_y	col_ang row_ang	lon	name
MFG (A)	1	2500	1250	0.0072	0°	grid_A.txt
MSG (S)	1	3712	1856	0.004803869	0°	grid_S.txt
MSF ARCH (A3)	3	833	416.333333	0.0216	0°	grid_A3.txt
MSG ARCH (S3)	3	1237	618.333333	0.014411607	0°	grid_S3.txt
GERB ARG	-	256	127.5	0.0703125	0°	grid_ARG.txt
GERB BARG	15	247	123.26666	0.072058035	0°	grid_BARG_SEV1.txt

9 Geolocation

The geolocation table contains, for each imager pixel, the geodetic latitude and longitude of the intersection of the imager line of sight (LOS) with the Earth's ellipsoid. Thanks to the rectification, the geolocation of the images disseminated by EUMETSAT is constant. The RMIB library program **create_geoloctable** is used to generate these tables from the grid parameters given in the previous section.

The geolocation tables are stored in files as a BATS library 'IP_images' structure (ROF binary format). To visualize the geolocation information, the **view_images** program can be used. For each format the geolocation table is also converted in a HDF file. For each imager/format a **disk flag image** is also computed that indicates if the LOS for a pixel intersects the Earth surface or not. Out of the Earth's disk (where the concept of latitude and longitude does not make sense), the latitude and longitude are set to 0.0.

The geolocation files are stored in the directory:

```
$DATA/Geolocation/\${FORMAT\}_GEOLOC.rof
$DATA/Geolocation/\${FORMAT\}_GEOLOC.hdf
$DATA/Geolocation/\${FORMAT\}_DISK.rof
```

The generation of a HDF5 file from the internal ROF format is performed using the utilitary program 'geoloc2hdf'

10 Imager acquisition time

The time of acquisition is available in the SEVIRI HRIT segment as the "L10LineMeanAcquisitionTime" in the "LineSideInfo" field and this information in copied in the XPIF files. For a given line, this time is different for each repeat cycle and is also different for all the spectral band (all the detectors are not at the same place in the focal plane). For the imager processing the acquisition time of each line is estimated from the time of the slot name t_{slot} (YYYYMMDDhhmm_MSG1...)) and the line index j (0:upper line, 3711: last bottom line) as:

$$c = \frac{j}{3711} \quad (20)$$

$$t = t_{slot} + (1-c)t_{top} + ct_{bot} \quad (21)$$

with the following mean values:

MFG	t_{bot} = -1800 s	t_{top}= -300 s
MSG	t_{bot} = 17 s	t_{top}= 759 s

11 Satellite Position

The position of the satellite should be know to compute the viewing zenith angle and the relative azimuth angle. In a first time this satellite is supposed to be on the Equator at the following fixed longitude:

```
MSG1 commissionning up to January 2004 = -10.5
MSG1 operation February 2004 onward    =  -3.4
MSG2 commissionning up to July 2006    =  -6.5
MSG2 operation August 2006  onward     =   0.0
```

In the future it is planned to use the actual satellite longitude provided in the HRIT prologue file.

12 Sun position and distance

The position of the Sun is needed to compute the solar zenith and the relative azimuth angle. This position is estimated using the BATS library routines:

```
D3_point LA _SunDirection(double t);
```

This routine is a (Bogdan-)modified version of the *Low precision formulas for the Sun's coordinates and the equation of time*, from the Astronomical Almanach 2002 (part C24). The routine gives the apparent coordinates of the Sun to a precision of 0.01^o and the equation of time to a precision of $0.1m$ between 1950 and 2050.

Additionaly, the Earth-Sun distance is needed to convert visible band radiance in reflectance. This distance is estimated using the BATS library routines:

```
double LA_EarthSunDistance(double t);
```

13 Spectral modeling parameters

The spectral modeling aims to estimate broadband radiances from NB radiance measurements. The BB radiances are the unfiltered radiances and the GERB filtered SW or LW radiances. In practice the BB radiance is estimated as a regression on the NB radiances where the coefficients of the regression are dependent on the viewing zenith angle θ_v (for thermal radiation) or solar zenith angle θ_s (for solar reflected radiation). More details about the method and performances are available in [TN05]. The parameterizations of the NB-to-BB regressions are done using the data base of spectral radiances fields at top of the atmosphere described in [TN30].

The spectral modelling parameters are computed using one of the following scripts:

```
/wind/nic/Unfiltering/MS5/batch.bat
/wind/nic/Unfiltering/MS7/batch.bat
/wind/nic/Unfiltering/Unfil_G2_SEV1
/wind/nic/Unfiltering/Unfil_G1_SEV2
```

The spectral modelling parameters are stored in the directory:

```
$DATA/SpectralMod/sm\_IMAGER\_QUANTITY\_ORDER.txt
```

where

- `IMAGER` specifies the imager : `ms5, ms7` or `seviri`,
- `QUANTITY` specifies the type of the NB-to-BB regressions (`sol, th, sw_sol, sw_th, lw_sol` or `lw_th`),
- `ORDER` is the order of the regression: `o1, o2` or `o3.`

Obviously, the regression coefficients should be recomputed in case of modification of the spectral response curves of the imager or of the GERB instrument.

14 Clouds Models

Radiative transfer computations

The STREAMER radiative transfer code has been used to compute the solar reflected radiance fields at the top of the atmosphere for different surfaces and for 2 types of clouds (water/ice) characterized by increasing cloud optical thickness. The mid-latitude atmospheric profile is used.

The different surfaces are (the internal spectral reflectance curves are used but are renormalized with the albedo given in the table):

surface	model	albedo	aerosol	surface identifier
ocean	1	default	Mar. + back.	`ocean`
bright desert	7	0.28	Tropo. + back.	`bright`
dark desert	10	0.20	Tropo. + back.	`dark`
lowtomod1	9	0.18	Tropo. + back.	`lowtomod`
lowtomod2	9	0.16	Tropo. + back.	
modtohigh1	11	0.15	Tropo. + back.	`modtohigh`
modtohigh2	12	0.15	Tropo. + back.	

The cloud features are:

	water	**ice**
z **cloud**	3-6 km	9-10 km
τ **cloud**	0-128	0-128
n_{re}	$12\mu m$	$70\mu m$ (hexagonal)

The convolution of the STREAMER bands with the weighting coefficients that correspond to different imager channels is done. The imager channels and the band weights are:

channel	identifier	STREAMER band	weighting coefficients
MS5 visible	`ms5_vis`	TBD	TBD
MS7 visible	`ms7_vis`	...	...
SEV1 0.6	`sev_06`	...	...
SEV1 0.8	`sev_08`	...	...
SEV1 HRV	`sev_hrv`	TBD	TBD
SEV2 0.6	`sev2_06`	TBD	TBD
SEV2 0.8	`sev2_08`	TBD	TBD
SEV2 HRV	`sev2_hrv`	TBD	TBD

Overcast reflectance model

The overcast situation is defined as corresponding to a cloud thickness of $\tau = 128$. In fact, overcast refers here to a very thick stratiform cloud. For each imager channel, we computed 5 (surface) * 2 (cloud phase) models that give the reflectance ρ as a generalized angular function:$\rho_{over} = \rho_{over}(\theta_v, \theta_s, \phi)$. The file are stored in:

```
$DATA/OvercastRef/overcastref_CHANNEL_SURF_PHASE.adm
```

where:

- `CHANNEL` is the channel identifier (`ms7_vis`, `sev_06`, ...),
- `SURF` is the surface identifier `(ocean, bright,` ...),
- `PHASE` is the cloud thermodynamic phase identifier (`water`, `ice`).

For example, for the MS7 visible channel, the 12 overcast models are stored in:

```
$DATA/OvercastRef/overcastref_ms7_vis_ocean_ice.adm
$DATA/OvercastRef/overcastref_ms7_vis_ocean_water.adm
$DATA/OvercastRef/overcastref_ms7_vis_modtohigh_ice.adm
$DATA/OvercastRef/overcastref_ms7_vis_modtohigh_water.adm
$DATA/OvercastRef/overcastref_ms7_vis_lowtomod_ice.adm
$DATA/OvercastRef/overcastref_ms7_vis_lowtomod_water.adm
$DATA/OvercastRef/overcastref_ms7_vis_dark_ice.adm
$DATA/OvercastRef/overcastref_ms7_vis_dark_water.adm
$DATA/OvercastRef/overcastref_ms7_vis_bright_ice.adm
$DATA/OvercastRef/overcastref_ms7_vis_bright_water.adm
```

The same files exists for the SEV1 VIS006 and SEV1 VIS008. Similar files should be derived for SEV2 (TBD).

Estimation of the cloud optical depth from the reflectance

For each imager pixel and each visible band channel, the "cloud amount" C is estimated by comparison of the actual reflectance ρ with the clear sky ρ_{cs} and overcast ρ_{over} reflectance values:

$$C = \frac{\rho - \rho_{cs}}{\rho_{over} - \rho_{cs}} \tag{22}$$

The clear sky reflectance ρ_{cs} is estimated by the weekly processing as described in [TN27,TN07]. The conversion from the cloud amount C to the cloud optical thickness τ is dependent on: the viewing geometry $(\theta_v, \theta_s, \phi)$, the imager channel ch, the cloud phase (water, ice) and the type of surface:

$$\tau = \tau(C, \theta_v, \theta_s, \phi, ch, phase, surf) \tag{23}$$

In practice a sigmoidal fit is used to convert C into τ:

$$\tau = \frac{\tau_0}{(A - \frac{B}{C})^{\chi}} \tag{24}$$

where the fit parameters τ_0, χ, A and B are dependent on the viewing geometry $(\theta_v, \theta_s, \phi)$ and the imager channel ch, the cloud phase $phase$ and the surface type $surf$. In practice, these parameters are stored as generalized angular function $f = f(\theta_v, \theta_s, \phi)$. These files are stored in:

```
$DATA/C2Tau/c2tau\_CHANNEL\_SURF\_PHASE\_tau0.adm
$DATA/C2Tau/c2tau\_CHANNEL\_SURF\_PHASE\_chi.adm
$DATA/C2Tau/c2tau\_CHANNEL\_SURF\_PHASE\_A.adm
$DATA/C2Tau/c2tau\_CHANNEL\_SURF\_PHASE\_B.adm
```

where `CHANNEL`, `SURF` and `PHASE` are the identifier described before.

15 Water Fraction Maps

A global coverage 1 km resolution land/water (binary) mask is available from the EDC DAAC web page:

```
http://edcdaac.usgs.gov/1KM/1kmhomepage.html
```

This mask is given as a raw flag image (40 031by 17 347pixels !) using an Interrupted Goode Homolosine Projection. A copy of this data is available in:

```
$DATA/LandMaskData/avhrr_land_mask.img.gz
```

Alessandro Ipe wrote a program `land_mask.c` that converts this binary image in a water fraction within the pixels of the geostationary satellite projection. The water fraction can be estimated because the imager pixel are greater than the 1km resolution of the land mask. This program and a batch file that calls it are:

The program takes as input the parameters of the rectified grid and creates the water fraction image as a U_CHAR image containing the percentage of water [0:100]% in the pixel.

From the water fraction image, an ocean flag image is constructed that indicates which pixels of the rectified grids are surely water. For this, the pixel and its 8 neighbours must have 100% water fraction. The ocean flag images are constrcuted using the `create_ocean_flag_im` program. The resulting data are:

```
$DATA/Surface/${FORM\}_WF.rof
$DATA/Surface/${FORM\}_OCEAN_FLAG.rof
```

Figure 6: Example of water fraction image (BARG_SEV1_WF.pgm).

16 Surface Type

IGBP Surface type Map

Global coverage maps of the International Geosphere Biosphere Programme (IGBP) are available from the USGS EROS Data Center (EDC) Distributed Active Archive Center (DAAC) page:

```
http://edcdaac.usgs.gov/glcc/glcc.html
```

2 Versions are currently vailable: version 1 (in fact 1.2) and version 2 (in fact 2.0). The data is given as a raw 1 byte/pixel huge image (40.031 by 17.347pixels !) using a "Interrupted Goode Homolosine Projection". Copies of these data (version 1.2 and 2.0) are available in:

```
$DATA/LandMaskData/gigbp1_2.img.gz
$DATA/LandMaskData/gigbp2_0g.img.gz
```

These maps give, for each 1 by 1km pixel, the IGBP class as given in Tab.(2).

Conversion in CERES-TRMM Surface type

The column "CERES" in Tab.(2) gives the associated CERES-TRMM surface code [2].

The program `igbp_mask.c` and script `create_ST.bat` are used to associate the IGBP class to CERES class and to project the 1km data in the various grids using the grid parameters given before and the Tab.(3). The program performs the post-discrimination between dark and bright desert using the CERES surface type (10') map provided by Norman Loeb. Fig.(7) shows the surface type image for the BARG format, after desert discrimination.

Value	Description	CERES
1	Evergreen Needleleaf Forest	2
2	Evergreen Broadleaf Forest	2
3	Deciduous Needleleaf Forest	2
4	Deciduous Broadleaf Forest	2
5	Mixed Forest	2
6	Closed Shrublands	2
7	Open Shrublands	4
8	Woody Savannas	2
9	Savannas	3
10	Grasslands	3
11	Permanent Wetlands	2
12	Croplands	3
13	Urban and Built-Up	4
14	Cropland/Natural Vegetation Mosaic	3
15	Snow and Ice	6
16	Barren or Sparsely Vegetated	5
17	Water Bodies	1
99	Interrupted Areas	-
100	Missing Data	-

Table 2: IGBP Land Cover Legend and associated CERES-TRMM surface type.

code	type	IGBP classes
1	ocean	17
2	mod-to-high Tree/Shrub cover.	1,2,3,4,5,6,8,11
3	low-to-mod Tree/Shrub cover.	9,10,12,14
4	dark desert	7,13
5	bright desert	16
6	snow	15

Table 3: IGBP surface type merging.

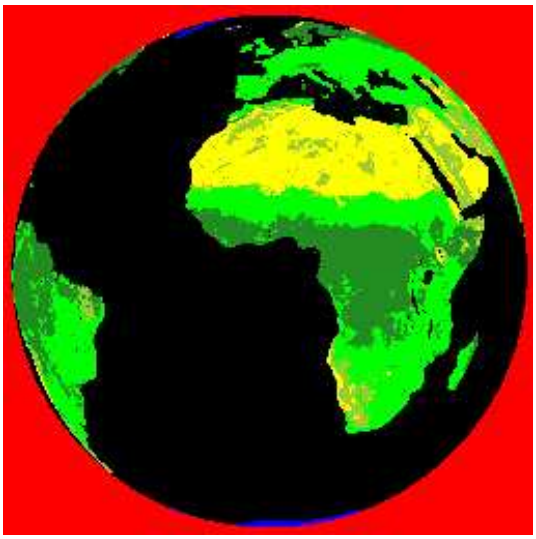

Figure 7: Surface type image after dark/bright desert discrimination (BARG_256_ST.pgm).

Bright/dark desert discrimination

The IGBP map is not sufficient to have a good discrimination between bright and dark desert. The 'desert' pixels in the images of surface type generated by the `igbp_mask` program are then post-processed using a surface map provided by the CERES team (10' resolution). This is done in the `igbp_mask` program provided that the option `-norman` is used. The CERES 10' map is located in:

```
$DATA/LandMaskData/ST_ceres_10m.pgm
```

The code in this image correspond to the one of Tab.(3).

Images of percentage of surface types

For the A3 and S3 formats (as well as the BARG format), the `igbp_mask` program also generates the images of the percentage of each CERES surface type in the footprints. For example, for the MFG A3 grid, those images are named:

```
$DATA/Surface/A3_ST_PERCENT_C0.rof  (\% of undefined)
$DATA/Surface/A3_ST_PERCENT_C1.rof  (\% of water)
$DATA/Surface/A3_ST_PERCENT_C2.rof  (\% of dark vege)
$DATA/Surface/A3_ST_PERCENT_C3.rof  (\% of bright vege)
$DATA/Surface/A3_ST_PERCENT_C4.rof  (\% of dark desert)
$DATA/Surface/A3_ST_PERCENT_C5.rof  (\% of bright desert)
$DATA/Surface/A3_ST_PERCENT_C6.rof  (\% of snow)
```

17 Wind Speed Climatology

The selection of clear ocean ADM is dependent on the wind speed. The climatology of the XXX project has been downloaded and regridded to the Meteosat projection. Monthly averaged data are available in files:

```
$DATA/WindSpeed/WS_{MONTH}-{GRID}.rof
```

where `MONTH` is the month and `GRID` the grid.

18 Shortwave CERES-TRMM Angular Dependency Models

Shortwave ADM

The Angular Dependency Models derived from the CERES instrument on the TRMM satellite are made available on the CERES Inversion Group home pages (plots and tables):

`http://asd-www.larc.nasa.gov/Inversion/`

Nevertheless, Norman Loeb and Dave Young provided us the code source for the SW radiance-to-flux conversion and also 4 files that contain the ADMs for 590 scenes:

admws.dat2b	Clear ocean
adm_groups.dat2b	Clear land
adm_ocecld.dat2b	cloud over ocean
adm_land_cld.dat2b	cloud over land

These files are specially interesting because the ADM association is done (that means that we do not have to deal with the "unsufficient data"). The program `trmm_read.c` reads these 4 files and generates the ASCII files for the 590 ADMs. The ADMs (albedo+bidirectional reflection function) are stored under a dedicated **ASCII format** in the directory:

`$DATA/ADM_CERES_TRMM/model_%04d.adm`

The meaning of the code [0:590] is provided on the web page:

`http://asd-www.larc.nasa.gov/Inversion/adm/trmm-adm-sw-type.tab`

The averaged model `mode_1001.adm` has also be computed and may be used when and where the scene identification is not possible or is dubious. The `adm_averaging.c` program is used to build the averaged model.

ADM Normalization

The normlisation is realized as explained in [3] with the data provided by the CERES team and stored in:

`$DATA/ADM_CERES_TRMM/ADM_TRMM_COR`

Clear ocean aerosol correction

Correction of the clear ocean ADM in case of important aerosol load can be performed using the data in:

`$DATA/ADM_CERES_TRMM/ADM_TRMM_COR/AERO`

This correction is not activated for the GERB-2 Edition-1 data.

19 ADMs for thermal radiation

The thermal angular dependency model is used to estimate the flux F_{th} from the thermal radiance L_{th} using:

$$F_{th} = \frac{\pi L_{th}}{R} \tag{25}$$

where the anisotropic factor R is dependent on the viewing zenith angle θ_v and on the kind of scene. More details are available in [TN08] and [1]. The parameterization of the models given hereafter are done using the data base of spectral radiances fields at top of the atmosphere [TN30]. The anisotropy is dependent on the NB radiances of the imager

$$R = R(\theta_v, \{L_{nb}\}) \tag{26}$$

In practice polynomial regression on the NB radiances $\{L_{nb}\}$ are used and the regression coefficients are dependent on the viewing zenith angle θ_v and are stored in the files:

```
$DATA/ADM/adm_thermal_ms5_o3.txt
$DATA/ADM/adm_thermal_ms7_o3.txt
$DATA/ADM/adm_thermal_seviri_o2_4inputs.txt
```

20 Aerosol retrieval

Helen dust detection

Helen Brindley designed a regression to discriminate between cloud and aerosol. The parameters are stored in the file

```
$DATA/Dust/reg_coeffs_ignatov_bt_wmoth.txt
```

Ignatov's LUT

Alexander Ignatov derived LUT to retrieve aerosol optical depth over cloud free ocean pixels for SEVIRI. These LUT are stored in the files:

```
$DATA/Dust/SEVIRI-Ch1-Lut-MLS-Ws_01.00-Wa_000-ang15
$DATA/Dust/SEVIRI-Ch2-Lut-MLS-Ws_01.00-Wa_000-ang15
$DATA/Dust/SEVIRI-Ch3-Lut-MLS-Ws_01.00-Wa_000-ang15
```

References

[1] N. Clerbaux, S. Dewitte, L. Gonzalez, C. Bertand, B. Nicula, and A. Ipe. Outgoing longwave flux estimation: Improvement of angular modelling using spectral information. *Remote Sensing of Environment*, 85:389–395, 2003.

[2] N. Loeb and S. Kato. Top-of-atmosphere direct radiative effect of aerosols over the tropical oceans from the clouds and the earth's radiant energy system (ceres) satellite instrument. *Journal of Climate*, 15(12):1474–1484, 2002.

[3] N.G. Loeb, N.M. Smith, S. Kato, W.F. Miller, S.K. Gupta, P. Minnis, and B.A. Wielicki. Angular distribution models for top-of-atmosphere radiative flux estimation from the clouds and the earth's radiant energy system instrument on the tropical rainfall measuring mission satellite. part i: Methodology. *Journal of Applied Meteorology*, 42:240–265, 2003.

Reference: Technical Notes

[**TN05**] Clerbaux, N. & Dewitte, S. (1999). RMIB GERB processing - SEVIRI processing : Spectral modeling. Reference Document MSG-RMIB-GE-TN-0005, RMIB.

[**TN07**] Clerbaux, N. & Dewitte, S. (1999). RMIB GERB processing - SEVIRI processing : Scene identification. Reference Document MSG-RMIB-GE-TN-0007, RMIB.

[**TN08**] Clerbaux, N. & Dewitte, S. (1999). RMIB GERB processing - SEVIRI processing : Angular dependency models. Reference Document MSG-RMIB-GE-TN-0008, RMIB.

[**TN29**] Clerbaux, N. (1999). Use of TIGR-3 atmospheric profiles as input for SBDART. Technical Note MSG-RMIB-GE-TN-0029, RMIB.

[**TN30**] Clerbaux, N. (1999). Generation of a data base of TOA spectral radiance fields. Technical Note MSG-RMIB-GE-TN-0030, RMIB.

[**TN36**] Clerbaux, N. (2003). Meteosat count versus ceres-trmm unfiltered radiance. Technical Note MSG-RMIB-GE-TN-0036, RMIB.